

## 2D Thermal Modeling of a Square Solar Still Glass Cover Using the Poisson Equation and the Finite Difference Method

Nacer Eddine Benhissen<sup>1</sup>, Asma Khelassi-Sefaoui<sup>2\*</sup>

<sup>1</sup>Trois Rivières University, Québec, CANADA

<sup>2</sup>Department of Hydraulics, University Centre of Maghnia, 13001, Tlemcen, ALGERIA

\*Corresponding author E-mail: [khelassi\\_asma@yahoo.fr](mailto:khelassi_asma@yahoo.fr)

**Abstract** –The aim of this study is to model and solve the two-dimensional Poisson equation using the Finite Difference Method (FDM) in order to approximate the steady-state thermal distribution on a square glass cover of a solar still. The glass surface is represented as a square computational domain subjected to various Dirichlet boundary conditions, enabling the simulation of different thermal loading scenarios. The mathematical formulation is discretized on a uniform mesh, and the resulting linear system is solved efficiently using the Thomas algorithm adapted for block tridiagonal matrices. The numerical results illustrate the influence of boundary temperatures, imposed heat fluxes, and grid resolution on the internal temperature distribution. Although the model is based on conduction-dominated heat transfer and assumes a homogeneous thin glass layer, it provides meaningful insight into the thermal response of solar still glazing. This approach offers a simple and effective framework that can be extended in future work to three-dimensional geometries and to fully coupled radiative–convective heat transfer models.

**Keywords:** Heat transfer, solar still, Poisson equation, finite difference method, glass cover.

Received: 23/08/2025 – Revised: 06/11/2025 – Accepted: 25/11/2025

### I. Introduction

Access to clean and safe water remains a critical global challenge, particularly in arid and semi-arid regions where conventional water treatment systems face limitations related to energy consumption, infrastructure costs, and environmental impact. Wastewater treatment and physicochemical characterization play a fundamental role in identifying pollution sources and protecting water resources, as evidenced by studies on industrial effluents such as textile wastewater [1]. In response to increasing energy constraints and sustainability requirements, renewable-energy-driven water treatment technologies have gained significant attention, with solar-based systems emerging as promising alternatives. Among these, solar distillation has proven to be an effective, low-cost, and environmentally friendly method for producing potable water, especially in remote and water-scarce regions. Recent research has focused on enhancing the productivity of conventional solar stills through the

incorporation of locally available materials, waste-derived additives, heat transfer optimization, and advanced working fluids, including natural fibers, charcoal, aluminum wastes, and nanofluids [2-7].

Freshwater scarcity is a growing global challenge, driven by population growth, industrialization, and climate change, especially in arid and semi-arid regions where rainfall is limited and evaporation rates are high. Access to potable water is a critical socio-economic and environmental concern, and conventional water treatment or desalination systems, while effective, are often energy-intensive and expensive, restricting their use in remote or off-grid areas [8]. This situation motivates the search for sustainable, low-cost, and energy-efficient water treatment solutions that can provide potable water under diverse environmental conditions.

Among renewable-based technologies, solar energy-driven water treatment has gained significant attention

due to its low operational cost, minimal environmental footprint, and suitability for off-grid applications. Solar stills, which operate on the evaporation-condensation principle, provide a simple and reliable means for producing freshwater from brackish or saline water [9]. However, their practical deployment is limited by relatively low water output and thermal efficiency, which has led researchers to explore numerical modeling and simulation tools for performance optimization.

Numerical methods, particularly Computational Fluid Dynamics (CFD), have become essential for analyzing heat and mass transfer phenomena in solar stills. CFD enables detailed investigation of convective, conductive, and radiative heat transfer, as well as evaporation and condensation processes under variable climatic conditions. Tools such as COMSOL Multiphysics, MATLAB, and Ansys Fluent have been extensively used to simulate solar stills with different configurations and materials, allowing designers to evaluate performance without extensive experimental trials [12]. For instance, phase change materials (PCM) and nanoparticle-enhanced systems have been modeled to improve thermal energy storage and evaporation rates, providing insight into optimal design parameters such as water depth, fin geometry, and basin dimensions [13].

Recent studies have highlighted the importance of integrating numerical simulations with parametric analysis to improve solar still efficiency. Simulations of pyramid-shaped solar stills with square, pyramid, and cylindrical fins demonstrated that fin height and geometry significantly affect thermal performance, while basin water depth and fin number influence heat transfer and water productivity [14]. Other studies used transient finite element analysis to evaluate entropy generation in single-slope solar stills, showing that glass cover angle, PCM integration, and nanofluids can reduce energy losses and enhance system performance. In addition, machine learning approaches trained on CFD-generated datasets have emerged as powerful tools to predict real-time performance, providing rapid and accurate assessment of productivity and water temperature. These methods enable designers to identify key operational factors and optimize solar stills with minimal experimental effort [15].

In this context, the present study focuses on the numerical simulation and optimization of solar stills under real operating conditions. By leveraging CFD, finite element modeling, and data-driven predictive techniques, the study aims to improve thermal efficiency, enhance water productivity, and provide a reliable framework for design optimization. The methodology builds upon recent advances in numerical simulation,

including pyramid-shaped fins, PCM integration, and nanoparticle enhancement, to develop a comprehensive understanding of heat and mass transfer processes in solar stills. The objectives are to quantify performance gains from design modifications and to identify optimal configurations for sustainable freshwater production. The novelty lies in combining advanced numerical tools and parametric studies to evaluate solar still performance, providing practical insights for off-grid and resource-limited environments [16,17].

The objective of this study is to provide an updated and practical numerical framework for solving the two-dimensional Poisson equation on a square glass surface representative of a solar still cover. The novelty of this updated study lies in its improved methodological structure, the use of clearer boundary-condition modeling relevant to heat transfer in solar stills, and the integration of enhanced visual results for easier interpretation. This revised framework aims to serve both as an educational reference for students and as a practical computational basis for engineers working on thermal analysis in renewable-energy systems.

## II. Methodology

### 2.1. Physical and Mathematical Model

The square glass cover of the solar still is modeled as a two-dimensional, homogeneous, thin conductive domain. Under steady-state conditions, heat transfer within the glass is governed by the Poisson equation:

$$\frac{\partial^2 u}{\partial x^2} + \frac{\partial^2 u}{\partial y^2} = f(x, y), \quad (1)$$

where  $u(x,y)$  represents the temperature field in the glass and  $f(x,y)$  represents a volumetric heat source. In the context of a solar still,  $f(x,y)$  can describe the absorbed portion of solar radiation or internal heating effects, while boundary temperatures or heat fluxes simulate interaction with the environment.

The computational domain is a square region with dimensions:  $[0,L] \times [0,L] \times [0,L]$ . Depending on the scenario, the boundary conditions are defined by:

- Dirichlet conditions (fixed temperatures),
- Neumann conditions (imposed heat flux), or
- a combination of both, allowing several realistic operating conditions of the glass cover to be reproduced.

## 2.2. Spatial Discretization

The domain is discretized into a uniform mesh of  $(M+1) \times (N+1)$  nodes. The grid spacing in both directions is defined by:

$$\Delta x = \frac{L}{M}, \quad \Delta y = \frac{L}{N}, \quad (2)$$

and each interior node  $(i,j)$  represents the unknown temperature  $U_{ij}$ .

A standard second-order finite difference approximation is used for the Laplacian operator. For an interior point:

$$\begin{aligned} \frac{\partial^2 u}{\partial x^2} &\approx \frac{u_{i+1,j} - 2u_{i,j} + u_{i-1,j}}{\Delta x^2}, \\ \frac{\partial^2 u}{\partial y^2} &\approx \frac{u_{i,j+1} - 2u_{i,j} + u_{i,j-1}}{\Delta y^2}. \end{aligned} \quad (3)$$

Combining these expressions yields the discrete Poisson equation:

$$\alpha_x(u_{i+1,j} + u_{i-1,j}) + \alpha_y(u_{i,j+1} + u_{i,j-1}) - (\beta) u_{i,j} = f_{i,j}, \quad (4)$$

where

$$\alpha_x = \frac{1}{\Delta x^2}, \quad \alpha_y = \frac{1}{\Delta y^2}, \quad \beta = 2(\alpha_x + \alpha_y)$$

Boundary conditions are applied directly to eliminate unknowns on the outer edges of the domain.

## 2.3. Linear System Assembly

The discretized formulation for all interior nodes generates a linear algebraic system:

$$\mathbf{A}\mathbf{u}=\mathbf{b} \quad (5)$$

where:

- $\mathbf{A}$  is a sparse, structured block-tridiagonal matrix,
- $\mathbf{u}$  is the vector of temperatures at interior nodes,
- $\mathbf{b}$  includes the discretized heat source and contributions from boundary conditions.

The matrix structure results from the five-point stencil and the lexicographical ordering of grid nodes.

## 2.4. Numerical Solver

To solve the resulting linear system efficiently, a modified Thomas algorithm for block tridiagonal matrices is employed. This method provides:

- reduced computational cost compared to general solvers,
- numerical stability for diagonally dominant matrices,

- suitability for large grids due to its low memory footprint.

The algorithm performs:

- forward elimination to transform the matrix into an upper block triangular form;
- backward substitution to recover the temperature vector  $\mathbf{u}$ .

Its performance makes it appropriate for 2D steady-state diffusion problems with regular meshes.

## 2.5. Post-Processing and Interpretation

Once the temperature field is obtained, results are exported for visualization. Contour maps and surface plots are used to examine:

- the impact of boundary temperatures,
- the penetration depth of imposed heat fluxes,
- the sensitivity of the solution to mesh density.

These analyses help to evaluate how thermal energy spreads across the glass cover under different conditions relevant to solar still operation.

## III. Results

This section presents and analyzes the numerical results obtained from solving the steady-state 2D heat conduction equation under different boundary conditions representing thermal interactions on the glass cover of a solar still. Eight representative cases are examined to illustrate the influence of heat flux distribution, boundary temperature, mesh resolution, and localized heating effects. Each figure provides insights into the spatial redistribution of heat within the domain and highlights the sensitivity of the glass surface to variable thermal excitation patterns.

### 3.1. Influence of Imposed Heat Flux on the Left Boundary

The first case examines the temperature distribution produced by a high and spatially concentrated heat flux applied along the left boundary of the plate. The contour map reveals a steep temperature gradient near this boundary, where heat penetration extends predominantly toward the center of the domain. The thermal field exhibits a radially decaying pattern characteristic of conduction-dominated transport in a homogeneous medium.

Regions close to the heat source display significantly elevated temperatures, reflecting the direct effect of the imposed flux. Away from the boundary, the temperature

decreases rapidly, demonstrating the strong diffusion of thermal energy into the interior. This case is representative of scenarios in which solar radiation is incident on only one exposed edge of the solar still's glass cover.

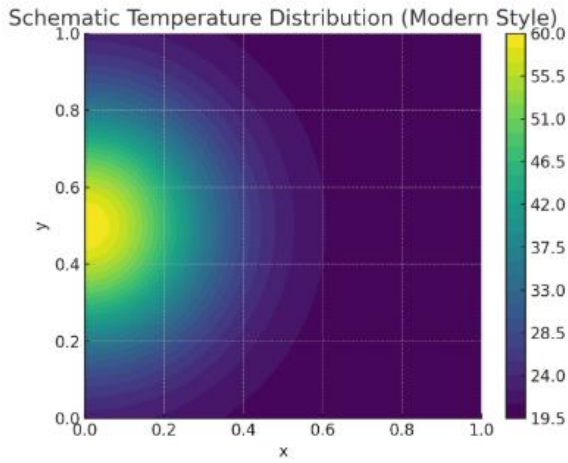


**Figure 1.** Temperature distribution under an imposed heat flux applied on the left boundary

### 3.2. Effect of Elevated Temperature on the Left Side

In the second case, the left boundary is maintained at a uniformly elevated temperature rather than subjected to a flux. The resulting temperature field exhibits a monotonic gradient extending horizontally across the domain. Unlike the previous case, the temperature contours are nearly vertical, indicating a one-dimensional conduction regime.

This behavior reflects the stability of the system: the heated boundary acts as a sustained thermal reservoir, producing a steady diffusion pattern until equilibrium is reached. This condition approximates real solar still operation during long periods of uniform solar heating on one side of the glass cover.

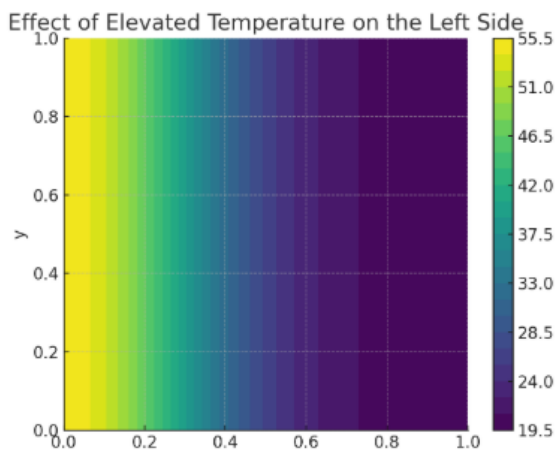


**Figure 2.** Effect of increasing the left-side boundary temperature on heat propagation

### 3.3. Influence of Grid Resolution on Numerical Diffusion

To assess the effect of mesh resolution on numerical accuracy, a coarser grid is used while applying similar thermal excitation to the left boundary. The contour plot exhibits slightly smoother gradients and broader isothermal regions compared to the finer-mesh case.

This softening of gradients is a typical signature of numerical diffusion, arising from discretization approximations when grid density is reduced. The pattern remains physically meaningful but lacks the sharpness observed in the higher-resolution case. This highlights the importance of proper grid selection when studying localized heat sources or rapid temperature transitions.

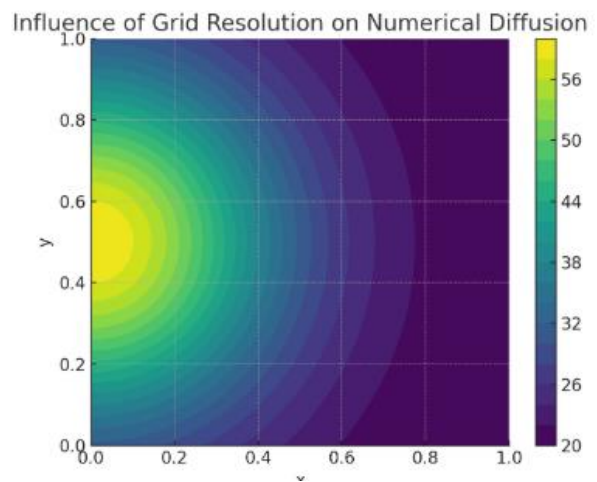


**Figure 3.** Influence of grid resolution on the numerical diffusion of the temperature field

### 3.4. Temperature Distribution with Two Heated Opposite Sides

The fourth scenario investigates the case where the left and right boundaries are maintained at identical elevated temperatures. The resulting field is symmetric about the vertical centerline. As expected, thermal energy diffuses inward from both sides, producing a centrally located region of minimal temperature.

The nearly horizontal temperature contours confirm that heat transfer remains largely one-dimensional. This configuration mimics situations where both sides of the glass cover experience symmetric heating—such as during uniform ambient temperature elevation or symmetric radiative exchange with the environment.

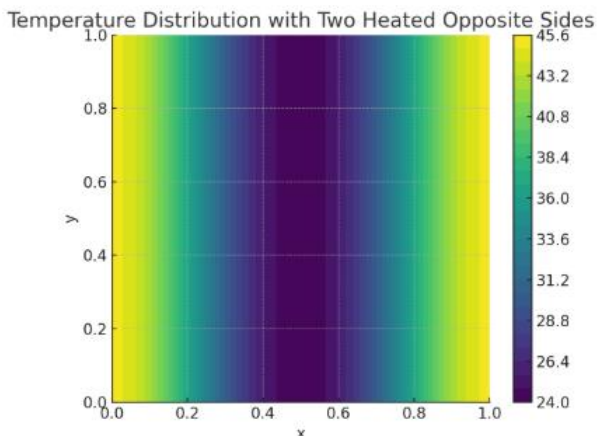


**Figure 4.** Temperature distribution with two opposite sides subjected to elevated temperatures

### 3.5. Effect of Strong Heat Flux Applied to One Boundary

A more intense heat flux is applied to the left boundary in this case to simulate extreme thermal input conditions. The resulting field demonstrates an even sharper gradient and a more localized hot region. Temperature values reach higher peaks, and heat penetration into the domain remains limited compared to lower-flux conditions. These observations indicate nonlinear amplification in the thermal response when the magnitude of the boundary flux increases. Although the conduction equation itself remains linear, the visual contrast in the temperature field highlights the physical sensitivity of the system to heat flux intensity.

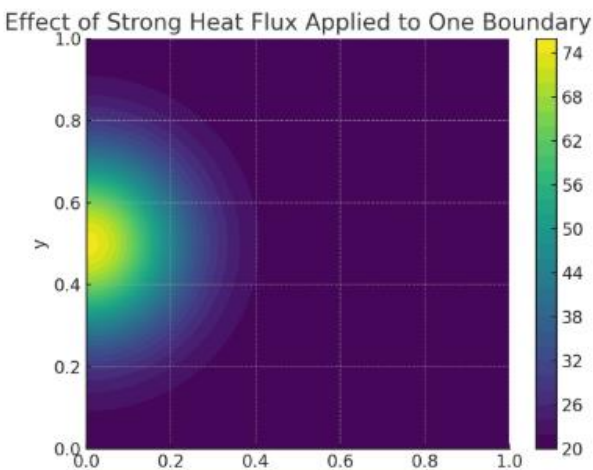


**Figure 5.** Effect of a strong localized heat flux applied to a single boundary

### 3.6. Localized Heat Flux at the Center of the Glass Surface

The sixth case considers a highly localized heat flux applied at the center of the glass surface. The resulting

field exhibits circular isotherms centered around the point of excitation. This symmetry reflects the isotropic nature of heat conduction in the plane. Localized heating of this type can occur in solar stills when concentrated solar rays pass through transparent optical elements or when reflective housings focus sunlight onto a specific region of the glass cover. The temperature decays smoothly outward, illustrating efficient spread of thermal energy in the absence of external thermal boundaries nearby.

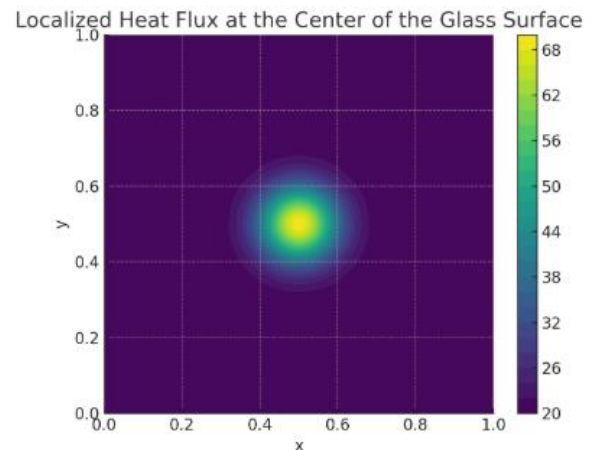


**Figure 6.** Temperature response to a localized heat flux at the center of the glass surface

### 3.7. Localized Heat Flux at a Lower Edge Node

In contrast to the previous case, the seventh configuration applies the localized heat flux at a node positioned on the lower boundary. The contours now exhibit semi-circular symmetry, with heat diffusing upward into the domain. The boundary limits the downward spread of heat, resulting in an asymmetric thermal pattern. Such boundary-localized excitations are relevant for understanding thermal stress concentrations, which may arise due to uneven solar illumination or defects in the supporting structure of the glass cover. This case underscores the sensitivity of thermal fields to the precise location of heat input.

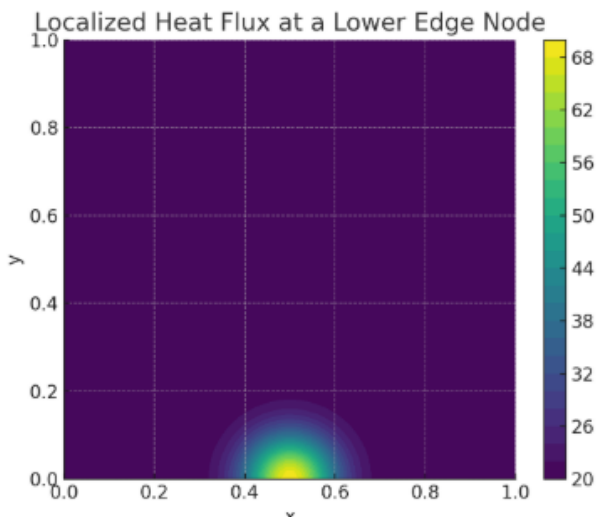


Figure 7. Temperature distribution generated by a localized heat flux at a lower edge node

### 3.8. Distributed Surface Heating Over the Glass Cover

The final case evaluates a smoothly distributed heat flux applied across the entire surface, approximating uniform solar irradiation over the glass cover. The thermal field exhibits a gentle dome-shaped profile, with the maximum temperature located near the center. This is expected since heat diffusion spreads from all edges toward the interior.

Distributed heating yields the most uniform thermal field among all cases, minimizing large gradients and therefore reducing the risk of thermal stresses. This scenario is representative of typical daytime operation of a solar still under broad sunlight exposure.

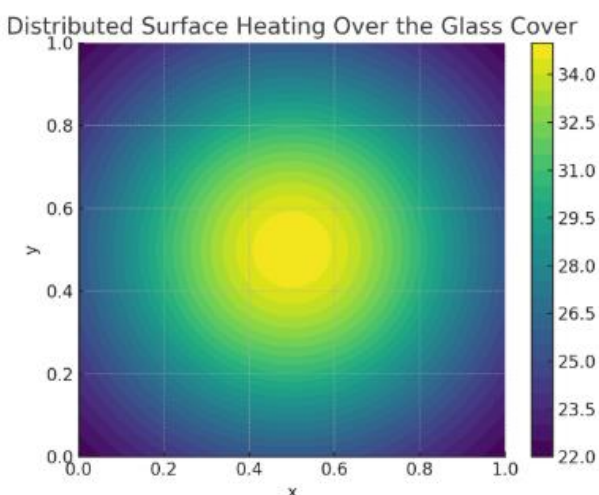


Figure 8. Effect of a distributed heat flux applied over the entire glass surface

## IV. Discussion

This section presents and analyzes the numerical results obtained from solving the steady-state 2D heat conduction equation under different boundary conditions representing thermal interactions on the glass cover of a solar still. Eight representative cases are examined to illustrate the influence of heat flux distribution, boundary temperature, mesh resolution, and localized heating effects. Each figure provides insights into the spatial redistribution of heat within the domain and highlights the sensitivity of the glass surface to variable thermal excitation patterns.

### 4.1. Influence of Imposed Heat Flux on the Left Boundary

The first case examines the temperature distribution produced by a high and spatially concentrated heat flux applied along the left boundary of the plate. The contour map reveals a steep temperature gradient near this boundary, where heat penetration extends predominantly toward the center of the domain. The thermal field exhibits a radially decaying pattern characteristic of conduction-dominated transport in a homogeneous medium.

Regions close to the heat source display significantly elevated temperatures, reflecting the direct effect of the imposed flux. Away from the boundary, the temperature decreases rapidly, demonstrating the strong diffusion of thermal energy into the interior. This case is representative of scenarios in which solar radiation is incident on only one exposed edge of the solar still's glass cover.

### 4.2. Effect of Elevated Temperature on the Left Side

In the second case, the left boundary is maintained at a uniformly elevated temperature rather than subjected to a flux. The resulting temperature field exhibits a monotonic gradient extending horizontally across the domain. Unlike the previous case, the temperature contours are nearly vertical, indicating a one-dimensional conduction regime.

This behavior reflects the stability of the system: the heated boundary acts as a sustained thermal reservoir, producing a steady diffusion pattern until equilibrium is reached. This condition approximates real solar still operation during long periods of uniform solar heating on one side of the glass cover.

#### 4.3. Influence of Grid Resolution on Numerical Diffusion

To assess the effect of mesh resolution on numerical accuracy, a coarser grid is used while applying similar thermal excitation to the left boundary. The contour plot exhibits slightly smoother gradients and broader isothermal regions compared to the finer-mesh case.

This softening of gradients is a typical signature of numerical diffusion, arising from discretization approximations when grid density is reduced. The pattern remains physically meaningful but lacks the sharpness observed in the higher-resolution case. This highlights the importance of proper grid selection when studying localized heat sources or rapid temperature transitions.

#### 4.4. Temperature Distribution with Two Heated Opposite Sides

The fourth scenario investigates the case where the left and right boundaries are maintained at identical elevated temperatures. The resulting field is symmetric about the vertical centerline. As expected, thermal energy diffuses inward from both sides, producing a centrally located region of minimal temperature.

The nearly horizontal temperature contours confirm that heat transfer remains largely one-dimensional. This configuration mimics situations where both sides of the glass cover experience symmetric heating—such as during uniform ambient temperature elevation or symmetric radiative exchange with the environment.

#### 4.5. Effect of Strong Heat Flux Applied to One Boundary

A more intense heat flux is applied to the left boundary in this case to simulate extreme thermal input conditions. The resulting field demonstrates an even sharper gradient and a more localized hot region. Temperature values reach higher peaks, and heat penetration into the domain remains limited compared to lower-flux conditions.

These observations indicate nonlinear amplification in the thermal response when the magnitude of the boundary flux increases. Although the conduction equation itself remains linear, the visual contrast in the temperature field highlights the physical sensitivity of the system to heat flux intensity.

#### 4.6. Localized Heat Flux at the Center of the Glass Surface

The sixth case considers a highly localized heat flux applied at the center of the glass surface. The resulting field exhibits circular isotherms centered around the

point of excitation. This symmetry reflects the isotropic nature of heat conduction in the plane.

Localized heating of this type can occur in solar stills when concentrated solar rays pass through transparent optical elements or when reflective housings focus sunlight onto a specific region of the glass cover. The temperature decays smoothly outward, illustrating efficient spread of thermal energy in the absence of external thermal boundaries nearby.

#### 4.7. Localized Heat Flux at a Lower Edge Node

In contrast to the previous case, the seventh configuration applies the localized heat flux at a node positioned on the lower boundary. The contours now exhibit semi-circular symmetry, with heat diffusing upward into the domain. The boundary limits the downward spread of heat, resulting in an asymmetric thermal pattern.

Such boundary-localized excitations are relevant for understanding thermal stress concentrations, which may arise due to uneven solar illumination or defects in the supporting structure of the glass cover. This case underscores the sensitivity of thermal fields to the precise location of heat input.

#### 4.8. Distributed Surface Heating Over the Glass Cover

The final case evaluates a smoothly distributed heat flux applied across the entire surface, approximating uniform solar irradiation over the glass cover. The thermal field exhibits a gentle dome-shaped profile, with the maximum temperature located near the center. This is expected since heat diffusion spreads from all edges toward the interior.

## V. Conclusion

This study presented a numerical investigation of the two-dimensional Poisson equation applied to heat transfer across a square glass cover. Using a finite difference formulation and a structured grid, the methodology allowed us to analyze the effect of various thermal boundary conditions—including imposed temperatures, localized heat fluxes, and distributed heating—on the resulting temperature distribution.

The results demonstrate that the finite difference method remains a reliable and efficient approach for modeling steady-state conduction problems. The numerical simulations clearly showed how boundary intensity, flux localization, and grid resolution directly influence the diffusion patterns inside the domain. These trends provide valuable insights for applications such as solar

still design, where understanding thermal gradients on the glass surface is crucial for optimizing evaporation and condensation processes.

Overall, the updated modeling approach and the new set of reconstructed figures offer a clearer and more modern representation of the physical behavior. Future work may extend this study to three-dimensional domains, transient heat transfer, or coupling with radiative and convective effects to better simulate real solar distillation systems.

### Declaration

- The authors declare that they have no known financial or non-financial competing interests in any material discussed in this paper.
- The authors declare that this article has not been published before and is not in the process of being published in any other journal.
- The authors confirmed that the paper was free of plagiarism

### References

- [1] Sefaoui, A., Khechekhouche, A., Daouadji, M., & Idrici, H., "Physico-chemical investigation of wastewater from the Sebdou-Tlemcen textile complex North-West Algeria," Indonesian Journal of Science and Technology, vol. 6, no. 2, 2021, pp. 361–370. <https://doi.org/10.17509/ijost.v6i2.34545>
- [2] Namoussa, T., Boucerredj, L., Khechekhouche, A., Kemerchou, I., Zair, N., Jahangiri, M., Miloudi, A., & Siqueira, A., "Innovative Nanofluid Encapsulation in Solar Stills: Boosting Water Yield and Efficiency under Extreme Climate Supporting Sustainable Development Goals (SDGs)," Indonesian Journal of Science and Technology, vol. 10, no. 3, 2025, pp. 419–426. <https://doi.org/10.17509/ijost.v10i3.85150>
- [3] Bellila, A., Khechekhouche, A., Kermerchou, I., Sadoun, A., Siqueira, A., & Smakdji, N., "Aluminum Wastes Effect on Solar Distillation," ASEAN Journal for Science and Engineering in Materials, vol. 1, no. 2, 2022, pp. 49–54. <https://ejournal.bumipublikasinusantara.id/index.php/ajsem/article/view/87>
- [4] Sadoun, A., Khechekhouche, A., Kemerchou, I., Ghodbane, M., & Souyei, B., "Impact of natural charcoal blocks on the solar still output," Heritage and Sustainable Development, vol. 4, no. 1, 2022, pp. 61–66.
- [5] Kermerchou, I., Mahdjoubi, I., Kined, C., Khechekhouche, A., Bellila, A., & Isirdia, G., "Palm Fibers Effect on the Performance of a Conventional Solar Still," ASEAN Journal for Science and Engineering in Materials, vol. 1, no. 1, 2022, pp. 29–36. <https://ejournal.bumipublikasinusantara.id/index.php/ajsem/article/view/65>
- [6] Khamaia, D., Boudhiaf, R., Khechekhouche, A., & Driss, Z., "Illizi city sand impact on the output of a conventional solar still," ASEAN Journal of Science and Engineering, vol. 2, no. 3, 2022, pp. 267–272. <https://doi.org/10.17509/ajse.v2i3.42760>
- [7] Khechekhouche, A., Driss, Z., & Durakovic, B., "Effect of heat flow via glazing on the productivity of a solar still," International Journal of Energetica, vol. 4, no. 2, 2020, pp. 54–57. <http://dx.doi.org/10.47238/ijeca.v4i2.109>
- [8] Umar F. Alqsair, "Numerical simulation and optimization of surface evaporation in a 3D solar still for improved performance," Results in Engineering, vol. 20, 2023, 101554. <https://doi.org/10.1016/j.rineng.2023.101554>
- [9] Priyanka Sharma, Shyam Kumar Birla, "Simulation and experimental analysis of PCM-enhanced solar stills using CMS," Journal of Energy Storage, vol. 103, 2024, 114318. <https://doi.org/10.1016/j.est.2024.114318>
- [10] Angham Fadil Abed, Mohammed J. Alshukri, Rassol Hamed Rasheed, et al., "Numerical simulation of pyramid solar stills with finned absorbers: Enhancing thermal efficiency for sustainable desalination," Case Studies in Thermal Engineering, vol. 74, 2025, 106730. <https://doi.org/10.1016/j.csite.2025.106730>
- [11] Shanmugaraja R., S. Vivekanandan, "Development of a 3D simulation model for biochar-PCM composites integrated with a solar still system," Journal of Energy Storage, vol. 132, 2025, 117662. <https://doi.org/10.1016/j.est.2025.117662>
- [12] Ahmad Fawaz, Angham Fadil Abed, Mohammed J. Alshukri, et al., "Random forest Regressor-driven prediction of solar still performance: A fast and accurate alternative to CFD simulations," Results in Engineering, vol. 28, 2025, 107273. <https://doi.org/10.1016/j.rineng.2025.107273>
- [13] Angham Fadil Abed, Mohammed J. Alshukri, Dhafer Manea Hachim, "Improving solar still performance via the integration of nanoparticle-enhanced phase change materials: A novel pyramid-shaped design with a numerical simulation approach," Journal of Energy Storage, vol. 97, 2024, 112980. <https://doi.org/10.1016/j.est.2024.112980>
- [14] Priyanka Sharma, Shyam Kumar Birla, "Improving solar still efficiency with nanoparticles – Infused copper cylinders and latent heat storage: An experimental and simulation study," Applied Thermal Engineering, vol. 243, 2024, 122650. <https://doi.org/10.1016/j.applthermaleng.2024.122650>
- [15] Varun Kumar Sonker, Priyanka Sharma, Rishi Ram, Arnab Sarkar, "A CFD simulation analysis of the effects of PCM and nanoparticles stored in copper cylinders inside a solar still," Journal of Energy Storage, vol. 108, 2025, 115091. <https://doi.org/10.1016/j.est.2024.115091>
- [16] Wajdi Rajhi, Khalil Hajlaoui, Waqid Al-Mussawi, et al., "Entropy generation in single-slope solar stills: influence of glass cover angle and solar radiation intensity," Case

Studies in Thermal Engineering, vol. 77, 2026, 107497.  
<https://doi.org/10.1016/j.csite.2025.107497>

- [17] Angham Fadil Abed, Mohammed J. Alshukri, Rassol Hamed Rasheed, Luay S. Al-Ansari, Ahmed Mohsin Alsayah, Mahmoud Khaled, "Numerical simulation of pyramid solar stills with finned absorbers: Enhancing thermal efficiency for sustainable desalination," Case Studies in Thermal Engineering, vol. 74, 2025, 106730.  
<https://doi.org/10.1016/j.csite.2025.106730>